



Thermal stability of glycerol containing compounds from the biodiesel production chain

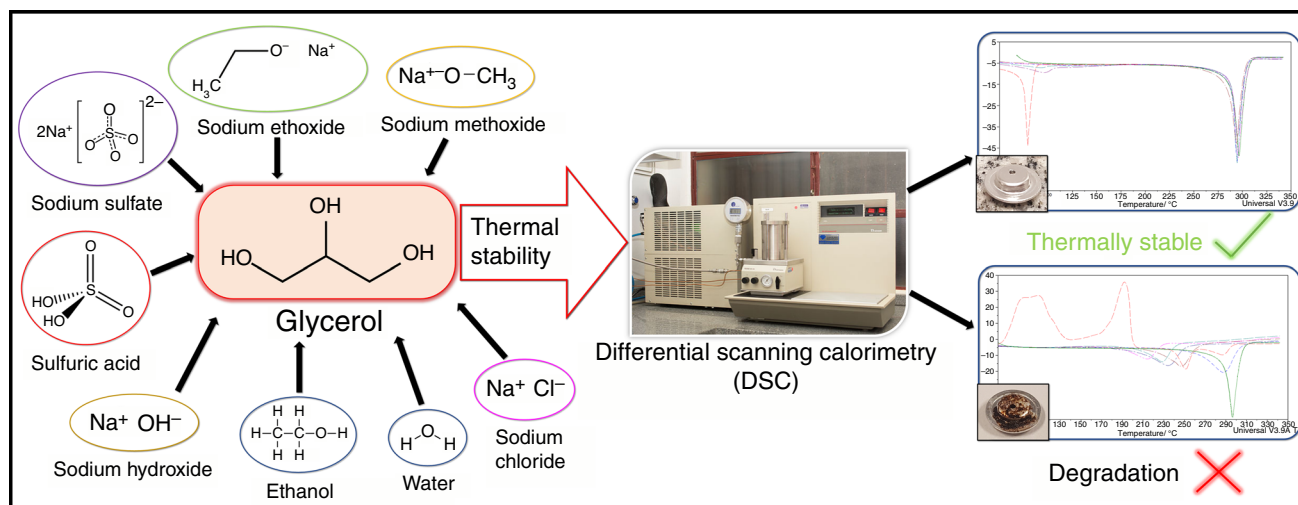
Daniel Gonçalves^{1,2} · Lilian Bozzi Barbeiro² · Patrícia Tonon de Souza² · Eduardo Augusto Caldas Batista² · Antonio José de Almeida Meirelles²

Received: 16 July 2021 / Accepted: 5 May 2022 / Published online: 8 June 2022
© Akadémiai Kiadó, Budapest, Hungary 2022

Abstract

Glycerol is a by-product from transesterification for biodiesel production. Due to the presence of hydroxyl groups (–OH), glycerol is pointed as a possible dehydrating agent for the production of anhydrous ethanol which, in turn, can be used as a methanol-substitute reagent in the transesterification. For that, glycerol must be purified by specific purification procedures, which are defined depending on the contaminant to be removed. In the case of thermal processes, as distillation, glycerol containing impurities from the biodiesel production must be thermally resistant to allow its reuse. The effect of some contaminants that can be found in glycerol was thus evaluated in terms of thermal stability of glycerol. Differential scanning calorimetry and thermogravimetry were used as tools to avail the thermal stability of several binary compositions of glycerol with a contaminant. Glycerol containing 5% sodium hydroxide or 5% sodium methoxide or 10% sodium ethoxide or sulfuric acid in any composition (up to 4.75%) exhibited a notable degradation. Therefore, it is required that the neutralization and further purifying steps ensure the removal of such contaminants or even to avoid the contact of glycerol with some dangerous compounds, as strong acids. On the other hand, the evaluated salts (sodium chloride and sodium sulfate) and water caused a change on the mixture boiling point, but no degradation was detected. Glycerol remained stable even containing high amount of ethanol or water (up to 30%), which confirms that such components can be removed from glycerol by thermal processes as distillation without its degradation.

Graphical abstract



Keywords DSC · Glycerin · Thermal behavior · Onset boiling temperature

Extended author information available on the last page of the article

Introduction

Significative environmental impacts caused by intensive use of fossil fuel and by-products, allied with their commercial value instability and depletion in a not-too-distant future, have stimulating the development of renewable energy sources [1]. Biofuels as bioethanol and biodiesel have been produced from waste materials and biomass from agriculture crops and industries [2]. Biodiesel is mostly produced by transesterification reactions of acylglycerols (mono-, di-, and triacylglycerols) with a short-carbon-chain alcohol, predominantly methanol due to its low cost and easy obtainment [3, 4]. However, methanol is mainly obtained from the upper vapor phase of petroleum distillation, being thus a non-renewable reagent with a high environmental impact involved.

Nowadays, Brazil takes over the technology of bioethanol production mostly from sugarcane juice fermentation, being the second main bioethanol producer worldwide [5, 6]. Ethanol has been intensively studied as a methanol substitute in the biodiesel production [7–12]. A possibility to obtain anhydrous or absolute ethanol (> 99.5%) is by the extractive distillation procedure [13, 14], in which a solvent with a high boiling point (or low volatility) is added to modify the relative volatility between ethanol and water, changing thus the azeotropic point. Glycols, as ethylene glycol ($C_2H_6O_2$), are effective in this specification, however glycerol ($C_3H_8O_3$), a by-product from the biodiesel refinery [1], must be highlighted for having a volatility (boiling point (BP) = 290 °C) lower than the one of ethylene glycol (BP = 197 °C) [15, 16] (peak temperatures). Therefore, the biodiesel production can be associated with ethanol dehydration by extractive distillation with glycerol as solvent, ensuring thus an integrated and “green process” of hydrous ethanol–biodiesel–glycerol–anhydrous ethanol production, as the patent proposed by Meirelles et al. [17].

However, the use of crude glycerol may cause some troubles to the process. It may contain insoluble salts and dissociated ions from the catalysts (oxides), their precursors (bases or acids), and neutralizer agents (also bases or acids) which, associated with high temperatures employed in distillation columns, may cause or accelerate the glycerol degradation and further generation of several compounds, including toxic ones. Besides that, insoluble/precipitated salts may incrust inside pipes and on the column bottom, acids or bases may damage equipment and accessories materials, leading thus to decreased process effectiveness and devices lifespan.

The degradation of impure glycerol at about 250 °C was first reported by Piękoś et al. [18]. Glycerol purification steps are indeed crucial to allow its reuse in the extractive distillation, or in several other processes. Ions can be

efficiently removed by ion exchange through anionic and cationic resins, without heating [17]. Ethanol and water can be removed by multistage distillation employing a maximum reboiler temperature of 250 °C, based on the results reported by Piękoś et al. [18]. This step is particularly more worrisome, since impure glycerol can be degraded under high temperatures, generating hazardous compounds, as acrolein [19], which is highly poisonous and extremely flammable [20]. Moreover, depending on the presence of specific compounds and conditions, glycerol can undergo several catalysis routes as reduction, oxidation, dehydration, etherification, esterification, acetalization, and so on, originating thus numerous compounds [21, 22].

In this sense, the evaluation of the thermal stability of impure glycerol is decisive to choose the required purification processes, as well to adjust or optimize their operational parameters. Moreover, a high-purity glycerol may afford the obtainment of several useful products from its glycolysis routes [21–23] or to make possible its incorporation into pharmaceutical products, as medicines and cosmetics formulations [22], free of toxic or hazard compounds.

More et al. [24, 25] mentioned some studies in which thermogravimetry (TG) and differential scanning calorimetry (DSC) were mainly used to evaluate the thermal behavior of vegetable oils and biodiesel. In general, mass losses by combustion, decomposition, and evaporation, thermal and oxidation stability were observed. More et al. [24, 25] also adopted these techniques to evaluate thermal behavior, besides the combustion process of biodiesel. Phase transitions as melting and evaporation, and oxidative stability can be both verified by DSC, a technique based on the difference of energy between a reference and sample as function of temperature and time [24, 25]. TG, in which the mass variation of sample is related to the temperature and time, can be usefully adopted on the evaluation of temperature stability and mass changes due to evaporation or decomposition (mass loss), or by oxidation (mass gain), for instance [24, 25].

This study aimed to evaluate the thermal stability of glycerol containing compounds from the biodiesel production process. For that, binary mixtures of glycerol and contaminant, namely water, ethanol, neutralizing compounds (sodium hydroxide and sulfuric acid), catalysts (sodium methoxide and sodium ethoxide), and salts (sodium chloride and sodium sulfate), were prepared with different mass proportions. The thermal behavior of mixtures was thus qualitatively evaluated by DSC technique, adopting two thermal tests (single run and cyclic). Some mixtures were also subjected to thermogravimetry (TG). Changes on DSC and TG curves were associated with thermal degradation, dissociation, oxidation, or phase transition (melting and/or

evaporation). Also, reaction routes were proposed for the mixtures in which degradation was identified.

Material and methods

Material

The provenance, supplier purity, and CAS numbers of each material here evaluated are shown in Table 1.

Contaminant selection

Glycerol, as a by-product from biodiesel production by transesterification reactions, may contain several impurities generated during the homogeneous catalysis using sodium hydroxide as a catalyst precursor, or from the direct employment of catalysts sodium methoxide or sodium ethoxide. Besides that, there is the possibility of contamination by strong acids as sulfuric acid employed in the neutralizing step, or for the reaction suspension, or even in esterification reactions, in where water and salts as sodium sulfate and sodium chloride are generated. Although glycerol is not generated during esterification, the ester containing sulfuric acid may be mixed with the products from the transesterification reactions. In this case, glycerol may be thus contacted with the acid.

The presence of ethanol in glycerol is unavoidable, since ethanol is used in excess to drive the reaction toward the biodiesel generation. Moreover, glycerol may contain water originated from neutralizing reactions, from hydrous ethanol, or even from esterification reactions, where free fatty acids are reacted with alcohol under acid catalysis, generating both ester (biodiesel) and water.

In this sense, the aforementioned compounds were selected as probable impurities or contaminants contained in the glycerol-rich stream. The effect of each impurity over the glycerol thermal stability and thermal behavior was thus qualitatively assessed by differential scanning calorimetry (DSC), in where changes on the baseline or in the glycerol boiling peak were monitored. Although crude glycerol may contain other compounds as free fatty acids, biodiesel, acylglycerols (mono-, di-, and triacylglycerols), their content is minor, being that such compounds were not considered here as possible contaminants.

Experimental procedure

Mixture preparation

Binary mixtures composed of glycerol and impurity at different mass compositions were prepared on an analytical balance (precision of 1×10^{-5} g, XP205, Mettler Toledo, USA). A certain mass of contaminant was added into a glass vessel

Table 1 Provenance, supplier purity, and CAS number of each material

Material	Provenance	Supplier purity ^a	CAS number	Molar mass/g mol. ⁻¹	Normal boiling point (NBP) ^b or melting point (MP) ^b of pure material/°C
Glycerol	Sigma-Aldrich/Merck, USA	> 99.5% (GC)*	56-81-5	92.09	290 (NBP)
Anhydrous ethanol	Merck, Germany	99.5% (GC)**	64-17-5	46.07	78 (NBP)
Sodium ethoxide	Sigma-Aldrich/ Merck, USA	95% (T, HCl)	141-52-6	68.05	
Sodium methoxide	Sigma-Aldrich/ Merck, USA	95% (T, HCl)	124-41-4	54.024	
Sodium hydroxide	Merck, Germany	≥ 99% (T, HCl)	1310-73-2	39.997	1388 – 1390 (NBP)
Sodium sulfate	Êxodo Científica LTDA, Brazil	≥ 99% (T, NaOH)	7757-82-6	142.04	884 (MP)
Sodium chloride	Merck, Germany	≥ 99% (T, AgNO ₃)	7647-14-5	58.44	800 – 801 (MP), 1412.8 (NBP)
Sulfuric acid	Qhemis, Hexis Científica, Brazil	> 95% (T, NaOH)	7664-93-9	98.08	290 (NBP)
Sodium ethoxide solution	Sigma-Aldrich/ Merck, USA	21%w sodium ethoxide in ethanol (T, NaOH)	141-52-6	49.42	
Water	Direct-Q, Millipore, USA		7732-18-5	18.015	100 (NBP)

^aFrom gas chromatography (GC) or titration (T) with HCl, NaOH, or AgNO₃, as informed by the supplier. Materials were used without further purification

^bPeak temperatures of normal boiling point (NBP, at 760 mmHg) or melting point (MP) [15, 16, 34]

*Moisture of $0.40\% \pm 0.01\%$ mass in glycerol was assessed by Karl Fischer titration (787 KF Titrino Plus, Metrohm, Switzerland) accoupled to an oven device (860 KF Thermoprep, Metrohm, Switzerland)

**Moisture of $0.26 \pm 0.01\%$ mass in anhydrous ethanol was assessed by Karl Fischer titration (787 KF Titrino Plus, Metrohm, Switzerland)

and then glycerol was added up to the desired composition. The vessel was immediately closed and the components were magnetically mixed until total homogenization. All mixtures were prepared under room conditions ($p = 945 \pm 10$ hPa, $T = 22 \pm 0.5$ °C, and atmospheric air). Vessels containing the mixtures were maintained closed at the dark under room conditions until sampling. Each compound mass and experimental mass percentage of the contaminant in the mixture can be accessed in Table 2.

Sampling

The DSC analysis was chosen as the main technique to evaluate the thermal stability of glycerol since it requires a low sample mass (~5 mg) and the results can be quickly obtained [26]. Phase transitions as melting and evaporation, and oxidative stability can be both verified by differential scanning calorimetry (DSC), a technique based on the difference of energy between a reference and sample as function of temperature and time [24, 25]. DSC curves also provide a fast qualitative result.

For that, a microanalytical balance (± 0.1 mg, AD-6, PerkinElmer, USA) was used for samples weighting. The device was daily calibrated by mass standards (10, 20, 100, and 200 mg, PerkinElmer, USA). Samples (2–5 mg) were carefully placed into a hermetic aluminum pan for DSC analysis with 25 μ L of internal volume (TA Instruments, Denmark). An empty pan was used as reference (*R*), and its mass was discounted from the pan used for sampling (*S*). Each *S* pan was selected assuming the minimum mass difference as possible from the *R* mass. After weighting, the sample pan (*S*) was cautiously sealed in a manual crimping tool for DSC pan (TA Instruments, Denmark), avoiding bad sealing or crumpled regions. Both *S* and *R* pans were thus allocated on their respective positions inside the DSC cell. Two analyses were carried out: glycerol thermal stability and boiling point (BP) assessment under a single heating run (Test 1), and thermal stability of glycerol during heating and cooling cycles (Test 2).

For Test 1, the following systems were evaluated: (i) pure glycerol; mixtures of glycerol with: (ii) 1, 5, 10, and 20% water; (iii) 1, 5, 10, 20, and 30% ethanol; (iv) 1, 2, and 5% sodium hydroxide; (v) 0.5, 1, 3, and 4.75% sulfuric acid; (vi) 1, 5, and 10% sodium methoxide; (vii) 0.5, 1, 5, and 10% sodium ethoxide; (viii) 0.5 and 5% sodium chloride; (ix) 0.5 and 1% sodium sulfate; (x) 1, 5, and 10% solution ethanol + 21% sodium ethoxide (nominal mass percentage). DSC curves of each pure contaminant were also assessed.

For test 2, the following systems were assessed: (i) pure glycerol; mixtures of glycerol with (i) 5 and 10% sodium hydroxide; (ii) 0.5% sulfuric acid; 1, 5, and 10% sodium methoxide; (iii) 0.5, 1, 5, and 10% sodium ethoxide; (iv) 0.5, 1, and 5% sodium chloride; (v) 0.5% sodium sulfate

(nominal mass percentage). Mixtures with ethanol or water were not evaluated because sampling evaporation occurred, even inside a hermetic DSC pan.

DSC analysis

The differential scanning calorimeter apparatus (DSC, Model 2920, TA Instruments, Denmark) was calibrated according to the ASTM E967-08 method [27], from which the baseline, DSC cell constant, and temperature reading are then calibrated.

The calibration was periodically checked by indium (In) standard (purity > 99.99%), assuming the melting point at the extrapolated onset temperature of 156.6 °C, with a heating ramp of 10 °C/min, according to ASTM reference procedures [27, 28]. Relative deviations between measured and reported melting points were not higher than 0.5%. Based on the literature [26, 29], a heating (or cooling) rate of 25 °C/min was adopted either for test 1 or test 2, which allowed a fast result without quality losses.

For Test 1, a DSC pan with pinhole lid was used, permitting sample evaporation. A tungsten carbide (WC) sphere with a diameter (1.0 mm) slightly higher than the hole one (0.8 mm) was placed over it to avoid sample pre-vaporization [26, 30] that, in turn, may cause a peak enlargement and a low DSC curve quality.

DSC analyses were carried out inside a pressure DSC cell under room pressure (945 ± 10 hPa) and atmospheric air (oxidizing atmosphere). Samples were heated from the room temperature (~22 °C) up to 350 °C at 25 °C \cdot min⁻¹, guaranteeing the total volatilization of glycerol, since pure glycerol evaporates at 290 °C (peak temperature) [15, 16] under atmospheric pressure (Table 1). Changes either in the baseline of the DSC curve or in the boiling peaks, mainly of glycerol, were thus evaluated. Each mixture was analyzed at least in triplicate. For that, at least three pans of each mixture were prepared and analyzed in a single-run, since for Test 1 occurred sample volatilization. Boiling points of the mixture or of the pure compound were calculated by the mean value of the onset temperatures and standard deviations were estimated by Type A [31].

Conventionally, boiling temperatures attained by DSC analysis are assumed as the extrapolated onset temperature, which is defined by the intersection between the baseline tangent and the tangent to the transition peak (boiling) [29, 32, 33]. Note that the boiling point (BP) reported in the literature (Table 1) refer to the peak ones (temperature on the top of the transition peak) of the pure material. Slight discrepancies between experimental and reported boiling point may be related either to the method adopted (onset or peak temperature) or to differences in room atmospheric pressure.

For Test 2, hermetic DSC pans were used, avoiding thus sample evaporation. Thermal analyses were carried out in a

Table 2 Mixture compositions and glycerol onset boiling point temperatures (BP) under local atmospheric pressure ($p=945$ hPa)

Compound	Glycerol mass ^a /g	Contaminant mass ^a /g	Experimental %w of contaminant ^b	Nominal %w of contaminant	Observable deg-radiation?	Boiling point (BP) ^c /°C
Pure glycerol (Fig. 1a)			Pure		No	289
Water (Fig. 2a)	1.02316	0.00999	0.967	1	No	289
	0.63443	0.03363	5.034	5	No	276
	0.98566	0.10826	9.897	10	No	258
	0.60557	0.15240	20.11	20	No	245
	0.75108	0.30941	29.18	30	No	242
Ethanol (Fig. 2b)	0.63443	0.03363	Pure	100	No	98
	2.20101	0.02211	0.995	1	No	288
	0.49157	0.02575	4.978	5	No	284
	0.77832	0.08573	9.922	10	No	288
	0.41501	0.10330	19.93	20	No	289
Sodium hydroxide (Fig. 2c)	0.62668	0.26521	29.74	30	No	287
			Pure	100	No	75
	2.12886	0.02133	0.992	1	No	290
	0.81850	0.01638	1.962	2	No	275
	0.61864	0.03178	4.886	5	Yes	266
Sulfuric acid (Fig. 2d)			Pure	100	Yes	
	1.11217	0.00548	0.490	0.5	Yes	
	2.37076	0.02022	0.846	0.85	Yes	
	1.23506	0.01245	0.998	1.0	Yes	
	0.66770	0.02006	2.917	3.0	Yes	
Sodium methoxide (Fig. 2e)	0.59122	0.02950	4.753	4.75	Yes	
			Pure	100	Yes	
	1.02093	0.00512	0.499	0.5	No	286
	0.63889	0.00643	0.996	1	No*	284
	0.35651	0.01885	5.022	5	No*	266
Sodium ethoxide (Fig. 2f)	0.44958	0.04945	9.909	10	Yes*	
			Pure	100	Yes	
	1.12836	0.00560	0.494	0.5	No	286
	0.59501	0.00598	0.995	1	No	284
	0.55060	0.02865	4.946	5	No	268
Sodium chloride (Fig. 2g)	0.21044	0.02212	9.512	10	Yes	
			Pure	100	Yes	
	1.45619	0.00730	0.499	0.5	No	285
	0.55790	0.02952	5.025	5	No	296
			Pure	100	No	> 400
Sodium sulfate (Fig. 2h)	0.93436	0.00460	0.490	0.5	No	288
	1.47366	0.01462	0.982	1	No	289
			Pure	100	Yes**	
Ethanol+21% Sodium Ethoxide solution (Fig. 2i)	0.90685	0.00921	1.005	1	No	278
	0.45312	0.02296	4.823	5	No	271
	1.30869	0.14511	9.981	10	Yes	272
		Pure	100	Yes		

^aMass of glycerol and contaminant in the mixture preparation. The balance uncertainty is 0.00001 g

^bExperimental mass percentage of contaminant in the mixture (glycerol + contaminant). In the case of “pure”, the compound purity can be verified in Table 1. Standard uncertainty (u) of mass percentage (%w) is $u(\%w) = 0.001$

^cOnset boiling temperature. Standard uncertainty (u) of boiling point (BP) in terms of the extrapolated onset temperature is $u(\text{BP}) = 1$ °C

*A small endothermic peak was observed at about 135 °C (peak temperature), which was more prominent in the mixture with 10% sodium methoxide

**Formation of two endothermic peaks within 220 and 260 °C (peak temperatures)

standard DSC cell accoupled to a cooling system supplied by N_2 (TA Instruments, Denmark). Each sample was subjected to at least five cycles of heating/cooling at $25\text{ }^\circ\text{C}\cdot\text{min}^{-1}$ under atmospheric pressure ($945 \pm 10\text{ hPa}$) from about $70\text{ }^\circ\text{C}$ to a maximum temperature of about $250\text{ }^\circ\text{C}$, which were based on the top and bottom temperatures of the distillation column for glycerol purification, as proposed by Meirelles et al. [17]. Glycerol stability was evaluated when exposed to consecutive heating and cooling steps, in a qualitative simulation of the glycerol stream thermal behavior during its reuse in the distillation multistage columns, assuming a reboiler/bottom temperature of $250\text{ }^\circ\text{C}$ and a top temperature of about $70\text{ }^\circ\text{C}$. Changes on the DSC curves during the cycles were thus appraised. Since there is no evaporation throughout Test 2 (hermetically closed system), it is not expected the presence of any peak.

Thermogravimetry

Glycerol with the following contaminant contents were also subjected to the thermogravimetric analysis (TG): 10% sodium hydroxide, 10% sodium methoxide, 5% and 10% sodium ethoxide. Such mixtures were chosen to confirm the degradation observed in DSC analysis. TG analysis were carried out by *Central Analítica* (Chemistry Institute – IQ, University of Campinas, Brazil) within 25 to $500\text{ }^\circ\text{C}$ at a heating ramp of $10\text{ }^\circ\text{C}\cdot\text{min}^{-1}$ under oxidant atmosphere (air). 2–5 mg sample were placed inside an alumina pan for TG. Based on this analysis results, it is possible to verify mass variations during heating, which may be related to evaporation (mass loss) or compounds formation (mass gain).

Results

DSC curves of pure glycerol are shown in Fig. 1 for different thermal stability tests. Figure 2 brings all DSC curves from Test 1 of binary systems composed of glycerol with: water (Fig. 2a), ethanol (Fig. 2b), sodium hydroxide (Fig. 2c), sulfuric acid (Fig. 2d), sodium methoxide (Fig. 2e), sodium ethoxide (Fig. 2f), sodium chloride (Fig. 2g), and sodium sulfate (Fig. 2h), in different mass compositions. DSC curves of ternary system (glycerol with ethanol + 21% sodium ethoxide solution) are illustrated in Fig. 2i, whereas the DSC curve of each pure component is grouped shown in Fig. 2j. DSC curves from Tests 1 and 2 can be separately visualized and in a better definition in the Supplementary Material.

Figure 3 illustrates DSC curves from Test 2 of binary mixtures of glycerol with: sodium hydroxide (Fig. 3a), sulfuric acid (Fig. 3b), sodium methoxide (Fig. 3c), sodium ethoxide (Fig. 3d), sodium chloride (Fig. 3e), and sodium sulfate (Fig. 3f). Again, the binary mixtures of glycerol with ethanol or with water were not evaluated in Test 2 since the

high pressure inside the pan caused its rupture and, consequently, mass losses.

In each DSC curve from Test 1, the following aspects were considered and associated with a probable sample degradation: (1) changes either in the baseline or in the glycerol or mixture boiling peak; (2) the existence of other peaks besides those already expected (related to glycerol, ethanol, water or mixture evaporation); (3) aggressive changes in glycerol boiling peak (peak deformation or severe peak displacement). Aspects 2 and 3 also may be associated with the generation of other compounds, which may compromise or not the glycerol quality. In DSC curves from Test 2, changes in each cycle line were assessed. (Remember that in Test 2 there is no expected peaks related to transitions as melting, evaporation, crystallization, and so on.)

Conventionally, exothermic peaks, which are related to chemical reactions, degradation, or oxidation, are directed up, whereas endothermic peaks, regarding phase transitions as melting or evaporation, are direct down. Since all samples are liquid, there is expected only the presence of the evaporation/boiling peak during Test 1 and no peaks in Test 2, since in this case the system is hermetically closed. Changes on the baseline or the presence of peaks excluding that related to the evaporation one, or even expressive changes on the evaporation peak, were qualitatively associated with partial or complete sample degradation. Glycerol boiling point and observable changes on its thermal behavior are summarized in Table 2. The boiling points can refer to the evaporation of pure compound, of mixture (glycerol + contaminant), or even of another compound that was generated from chemical reactions of glycerol with contaminant.

Figure 4 brings TG curves (green lines) and derivative TG (DTG, blue lines) from thermogravimetric analysis. Peaks on the blue line directed up are related to thermal events, as phase transitions or reactions. Decay on the green curve is related to mass losses, whereas percentage on the black straight lines represent the percentage of lost mass in each event. TG and DTG curves can be separately visualized and in a better resolution in Supplementary Material.

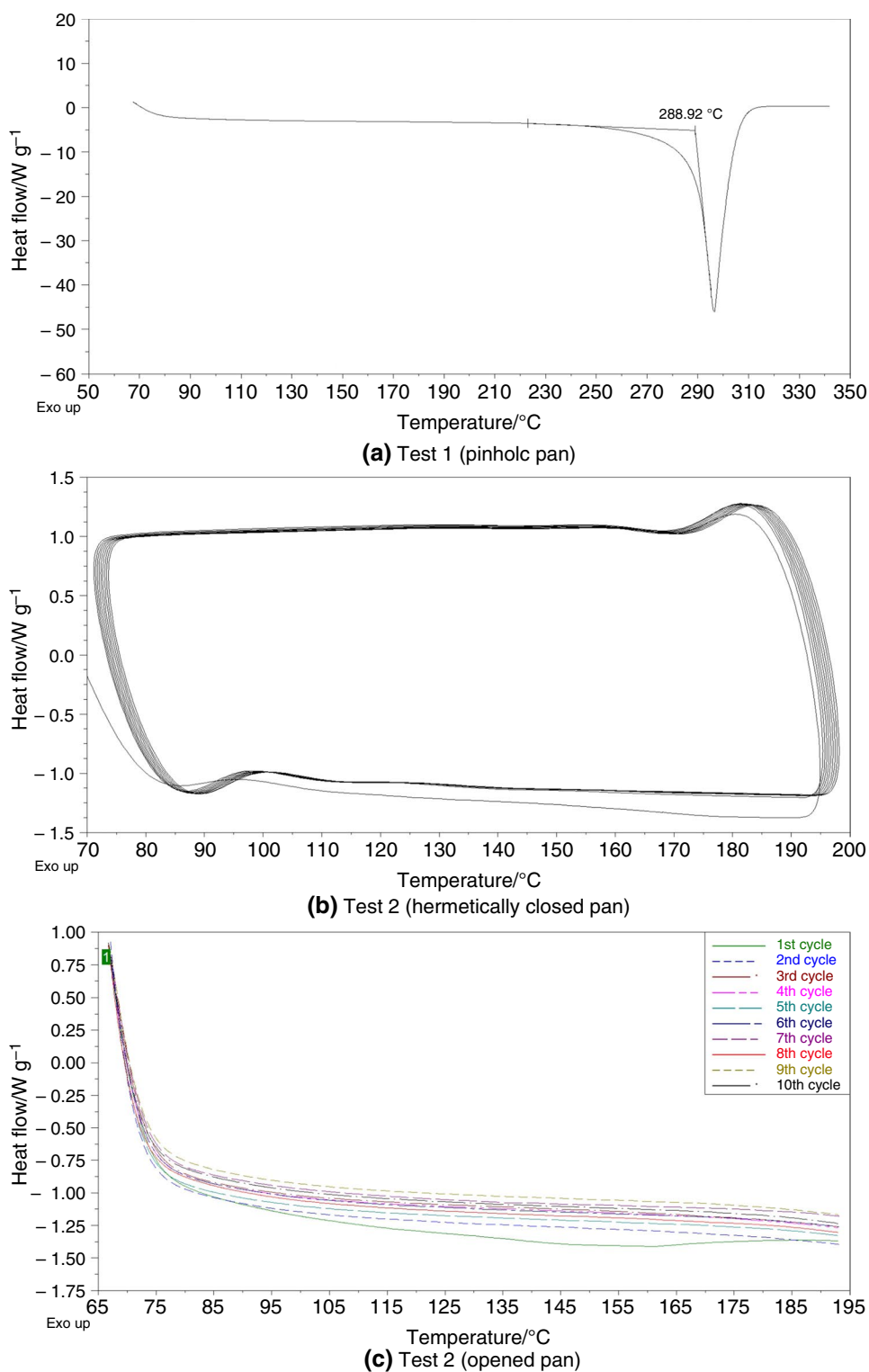
Discussion

Test 1: single run

Pure glycerol

The DSC curve of pure glycerol is represented either in Fig. 1 or in all images of Fig. 2. Pure glycerol maintained thermally stable throughout the heating until is completely evaporation (Fig. 1a). According to Castelló et al. [19], glycerol is thermally stable when exposed to the atmospheric air or nitrogen gas (inert atmosphere); therefore, there is no

Fig. 1 DCS curves from thermal tests of pure glycerol (99.5% purity)



expressive oxidation or degradation during heating. Boiling point (BP) of glycerol under atmospheric pressure estimated by the onset temperature was $BP = (289 \pm 1) \text{ } ^\circ\text{C}$ (Fig. 1a), which is in accordance with reported values ($290 \text{ } ^\circ\text{C}$) [15, 16, 19, 34]. Again, slight differences between experimental and reported boiling point may be related either to the

method adopted for the BP measurement (onset or peak temperature) or to the room pressure.

Finally, it was verified that either the DSC pan material (aluminum) or moisture (from sample or air) did not expressively affect the thermal stability of pure glycerol until its total evaporation.

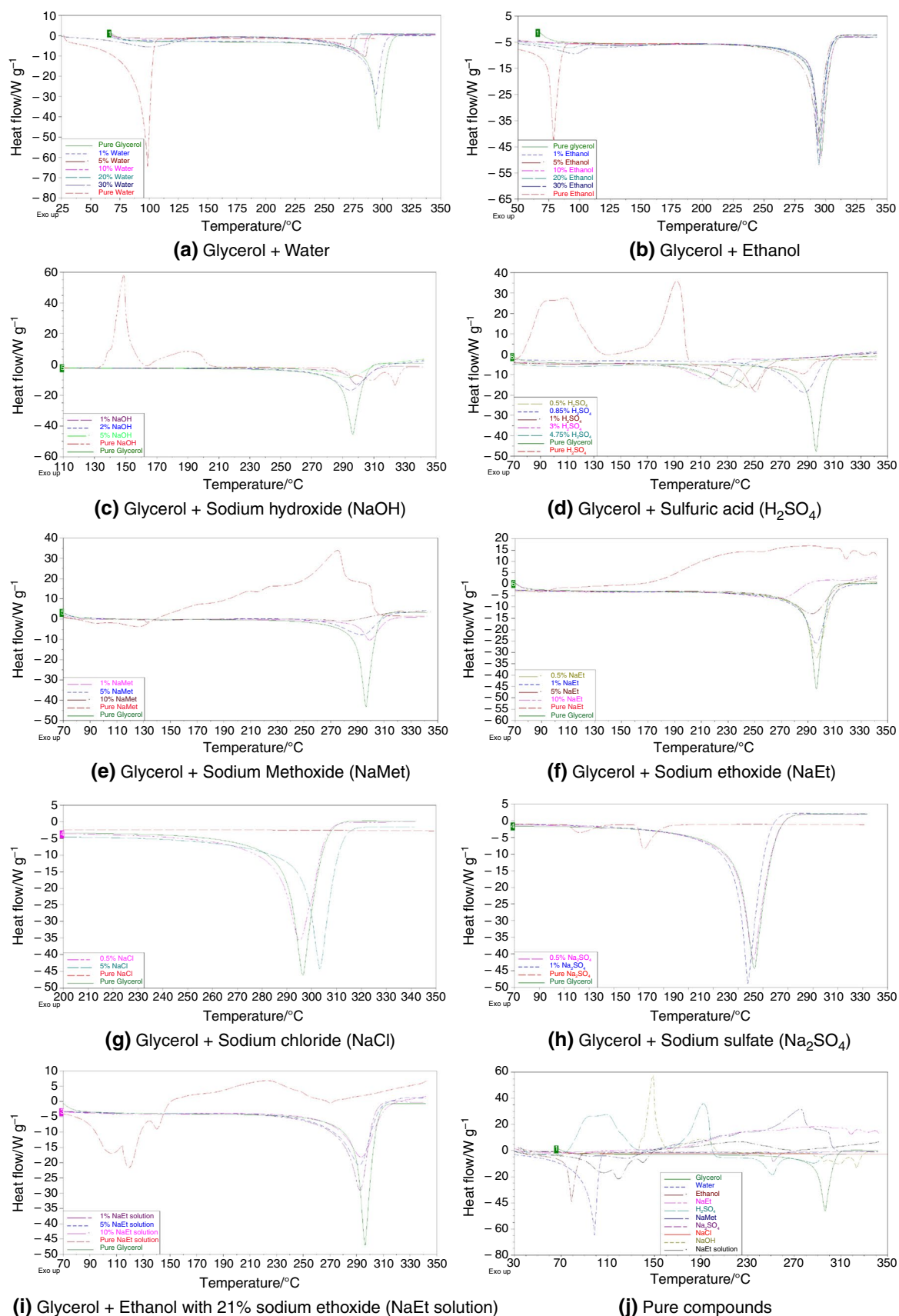


Fig. 2 DSC curves from Test 1 for mixtures of glycerol with contaminants in different compositions

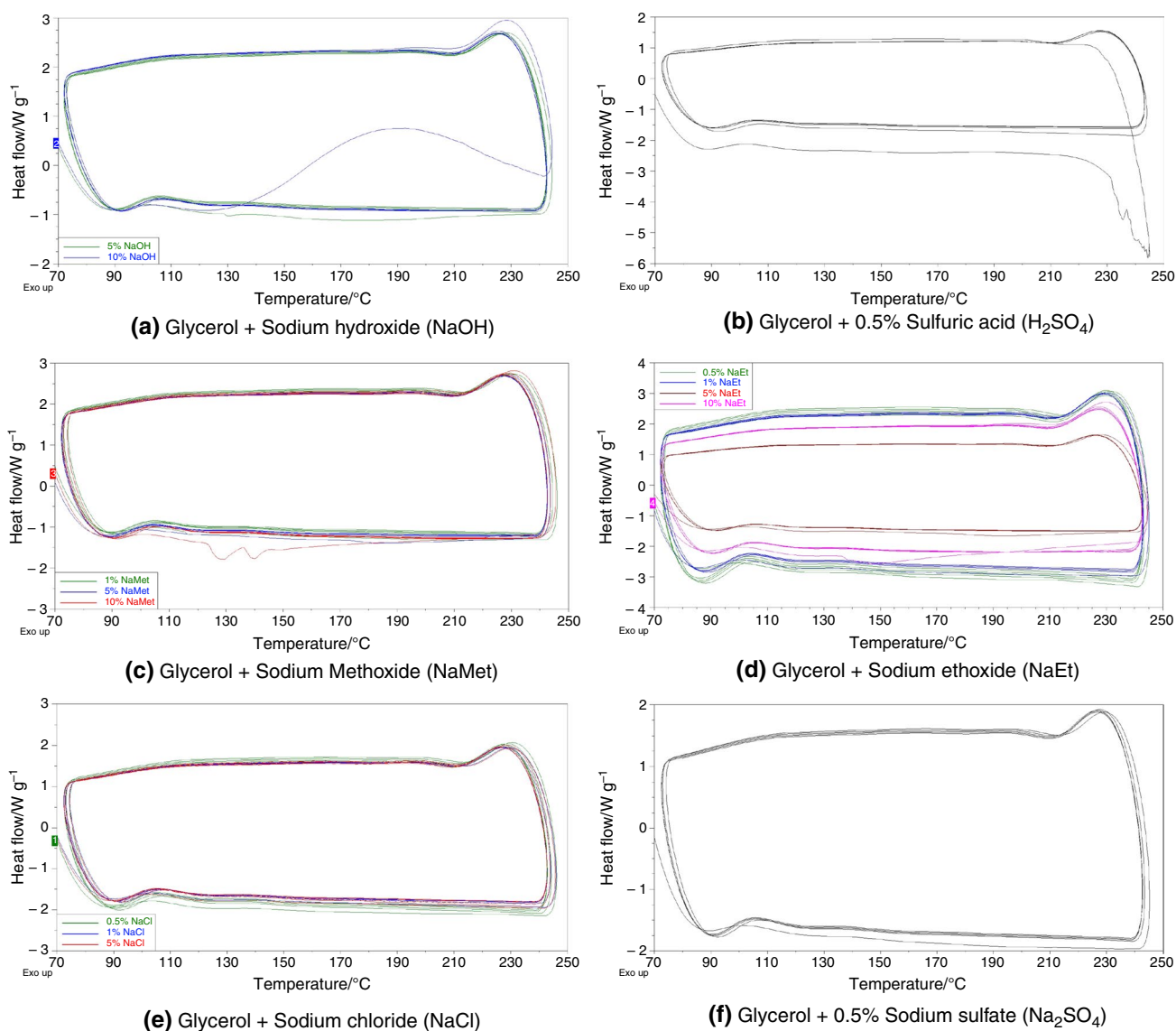


Fig. 3 DSC curves from Test 2 for mixtures of glycerol with contaminants in different compositions

Water

DSC curves for glycerol + water mixtures are displayed in Fig. 2a, where it is observable that increased water content in sample led to decreased boiling point of glycerol or of mixture (glycerol + water) (Table 2), since the evaporation peak was displaced toward left (see tall peaks after 245 °C). On the other hand, the peaks related to water evaporation were displaced toward right (see large peaks at the beginning of the heating run). Increased water content in the solution also caused an enlargement of both evaporation peaks, which is more prominent for water (see the large peak at the beginning of the run for glycerol + 30% water in Fig. 2a).

Glycerol and water are strongly linked through hydrogen bonds [35]. One glycerol molecule can reach up to

nine hydrogen bonds with another glycerol molecule or with water (an average of three bonds for each OH group), whereas only one water molecule has about 4 hydrogen bonds with another water molecules [36]. Jahn et al. [36] found that the number of hydrogen bonds decreases under heating. For glycerol, about 6–7 bounds were estimated at 27 °C, decreasing to 5–6 at 180 °C. The number of hydrogen bonds depends on the force field model approach adopted. Nevertheless, the intermolecular interaction between glycerol and/or water is weakened during heating.

While glycerol reduces the partial pressure of water [37], water in turn increases the glycerol partial pressure, affecting thus their boiling points. In other words, glycerol “holds” water in the liquid phase, whereas water “pulls” glycerol to the vapor phase. Despite those changes, there

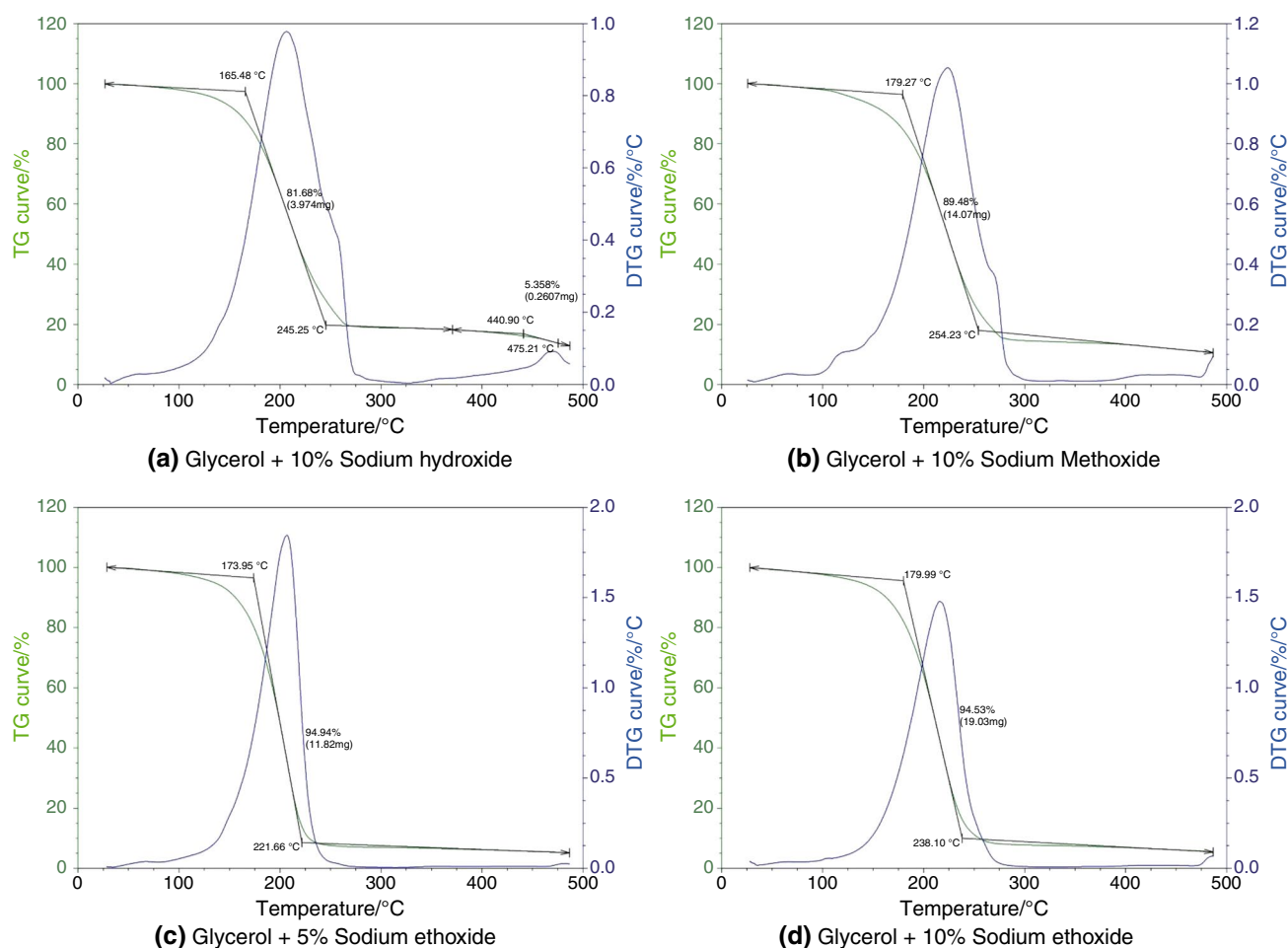


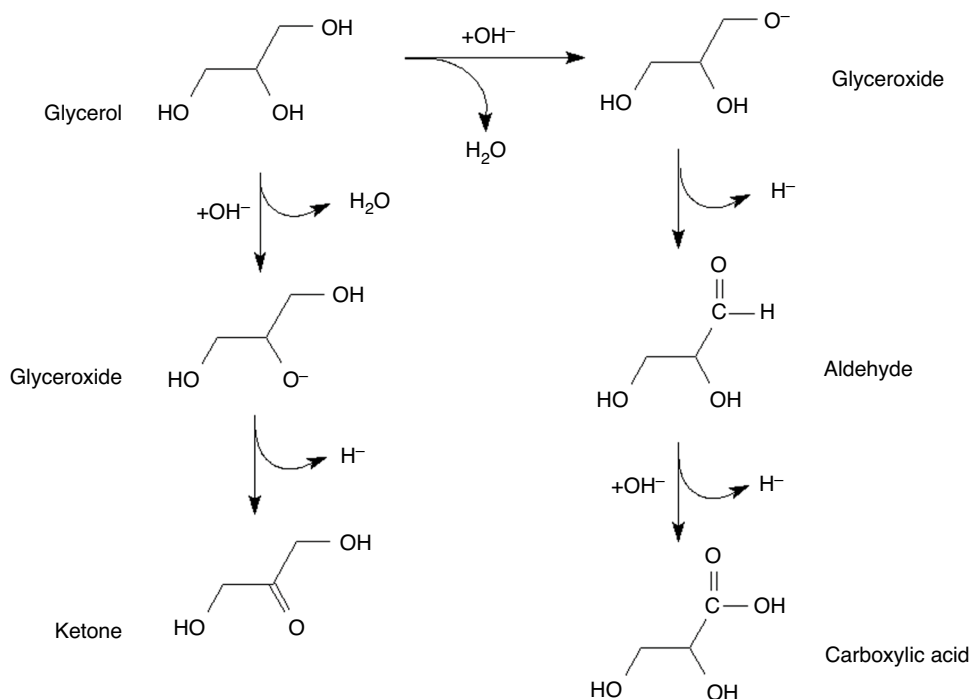
Fig. 4 Thermogravimetric results for mixtures of glycerol and contaminant. Green line: TG curve; blue line: DTG curve; black straight lines indicate the temperature range of thermal events (peaks in the blue line) and the correspondent mass loss

was not found any anomaly either on the baseline or in the evaporation peaks. Although water can catalyze some reactions, as dehydration, oxidation, hydrolysis, and so on, the mixture glycerol + water maintained stable even at high water composition (up to 30% in mass at least). Since the boiling point of glycerol changes according to the water content, the evaporation peak may be referred to a hydrated glycerol (glycerol + bonded water), not to the pure compound.

Glycerol proved to be thermally stable when containing water. Such impurity can be thus removed from glycerol by distillation with a bottom temperature lower than the one for glycerol evaporation (290 °C). Since the water found in glycerol leads to its expressive boiling point decreasing, the temperature on the column bottom must be controlled to be always lower than glycerol boiling point to avoid its evaporation.

Ethanol

DSC curves for glycerol + ethanol mixtures are shown in Fig. 2b. As in water, glycerol is also completely soluble in ethanol due to the formation of hydrogen bonds [19]. Glycerol also decreases the partial pressure of ethanol, leading to its increased boiling point (short peaks at the beginning of the heating run). However, ethanol almost did not affect the boiling point of glycerol (tall peaks after 250 °C). Although ethanol molar mass (46.07 g mol⁻¹) is higher than water (18.02 g mol⁻¹), the boiling point of pure ethanol is lower (78.2 °C [15]), which may be a result of a lower number of hydrogen bonds per volume. A hypothesis is that, although ethanol is completely soluble in glycerol, there is a lower number of intermolecular bonds per volume in a glycerol + ethanol mixture. Moreover, water has more hydrogen bonds than the OH group found in ethanol molecule [36]

Scheme 1: Glycerol oxidation by sodium hydroxide (NaOH)

making its effect over glycerol volatility more prominent than ethanol.

Although ethanol has a slight acid character, its acidity is too low ($pK_a = 15.9$) and the dissociation force is too weak to promote an expressive dehydration of glycerol. Therefore, as observed for water, glycerol maintained thermally stable when mixed with ethanol even at high ethanol composition (up to 30% in mass). For this reason, glycerol is a good option as solvent in the extractive distillation of hydrated ethanol [13, 14].

Moreover, likewise water, ethanol can be also removed from the glycerol stream in a multistage distillation, operating with a boiler temperature below the glycerol boiling point with no relevant changes on the chemical structure of glycerol. However, it is still necessary to evaluate how many times glycerol can be submitted to such process without its degradation (Test 2).

Alkali reagents

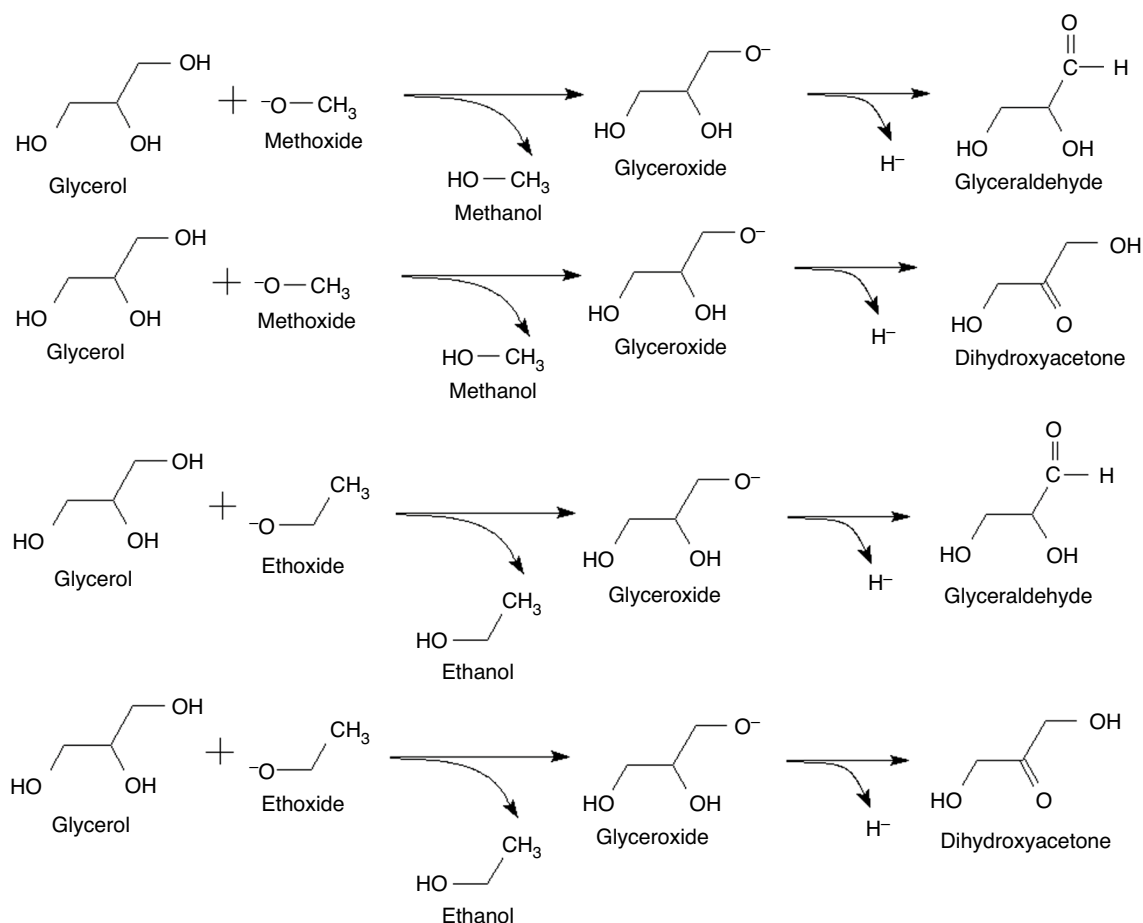
DSC curves for glycerol + sodium hydroxide, + sodium methoxide, and + sodium ethoxide mixtures are shown in Fig. 2c, e, and f, respectively, where it is possible to observe the sample degradation of some mixtures. In the case of these alkali reagents, glycerol undergoes several alkali reactions under metallic catalysts, generating aldehydes, carboxylic acids, carbonates, and diols [21, 38, 39]. Although there is no metallic catalyst in these systems, expressive changes on the DSC curves were observed, meaning that the sample was modified during the heating.

The main hypothesis is the dehydrogenation of glycerol by sodium hydroxide. The hydroxide unbound electrons pair (OH^-) of sodium hydroxide (NaOH) remove a proton (H^+) from hydroxyl group found in C1 or C3 of glycerol molecule, resulting in water and glyceroxide [40] (Scheme 1). The unbound electrons pair of glyceroxide (O^-) can dislocate to the adjacent carbon and form a carbonyl, originating an aldehyde. The OH^- from NaOH can also remove a proton from the central carbon of glycerol (C2), resulting in a ketone (Scheme 1).

Secondary oxidation compounds can be also generated in a condition of highly available oxygen, or high alkali reagent amounts. Therefore, in the experimental conditions of this study, the aldehyde group (CHO) may eventually be oxidated into its correspondent carboxylic acid (Scheme 1).

Another reaction routes of glycerol dehydrogenation may occur under the presence of alkali reagents [39] as sodium hydroxide, sodium methoxide, and sodium ethoxide. Acid lactic can be also formed from glycerol hydrodeoxygenation by sodium hydroxide. The reaction is increased under heating and alkali reagent concentration [38]. However, such reactions occur under specific metallic catalysts that are not present in the system.

Regarding pure sodium hydroxide, both endothermic and exothermic peaks were observed in its DSC curves (Fig. 2c). Endothermic peak at about $320\text{ }^\circ\text{C}$ (peak temperature) may be associated with the compound melting (sodium hydroxide melting point = $318\text{ }^\circ\text{C}$ [15], expressed as peak temperature under 760 mmHg), whereas exothermic peaks at $150\text{ }^\circ\text{C}$ and $190\text{ }^\circ\text{C}$ (peak temperatures) may be related to



Scheme 2: Glycerol oxidation by sodium methoxide or sodium ethoxide

the dehydration of $\text{NaOH}\cdot\text{H}_2\text{O}$ followed by the formation of sodium oxide (Na_2O) and water vapor [41].

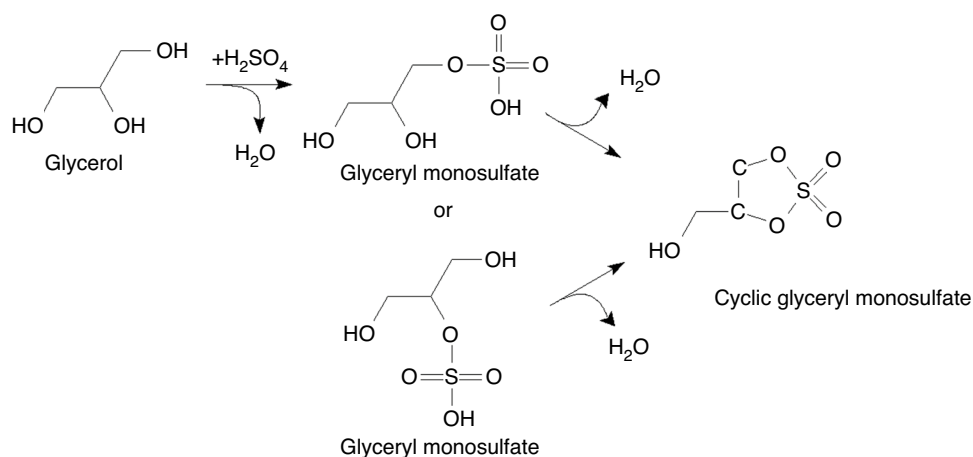
Alkali reagents as sodium methoxide and sodium ethoxide react with glycerol through similar mechanism to sodium hydroxide. The alkoxide (methoxide or ethoxide) can remove a proton (H^+) from the hydroxyl group of glycerol, resulting in alcohol (methanol or ethanol) and glycerinaldehyde or dihydroxyacetone (Scheme 2). Volatile compounds as methanol (boiling point = $64.7\text{ }^\circ\text{C}$) and ethanol (boiling point = $78.2\text{ }^\circ\text{C}$) may evaporate and thus affect the DSC curve.

In the case of pure compounds, sodium methoxide is a powder extremely instable when contacted with air and humidity, leading to its degradation from about $50\text{ }^\circ\text{C}$ [42]. At temperatures lower than $350\text{ }^\circ\text{C}$, sodium methoxide may react with the air humidity, resulting in vapors of methane (CH_4), followed by ethane (C_2H_6), and propene (C_3H_6), and also in solid compounds as carbonate, sodium hydroxide, and amorphous carbon [43]. Sodium ethoxide decomposition begins at temperatures lower than $300\text{ }^\circ\text{C}$, resulting mainly in the formation of ethene (C_2H_4), and minor amounts of

ethane (C_2H_6), propene (C_3H_6), and butene (C_4H_8), besides carbonate, sodium hydroxide, and amorphous carbon [43]. Moreover, evaporation of residual methanol or ethanol contained in the oxides may also occur.

Besides the aforementioned reactions between glycerol and sodium methoxide or sodium ethoxide, the decomposition of pure alkali reagents (sodium hydroxide, sodium methoxide, or sodium ethoxide) may have also contributed for changes on DSC curves of samples (Fig. 2c, e, f).

Comparing the DSC curves obtained for the three alkali reagents, it was observed a direct relation between the alkaline force and the compound effect over glycerol. The alkaline force is related to the dissociative force. Sodium hydroxide exhibits an alkaline dissociation constant or basicity ($pK_b = 0.2$) higher than sodium methoxide and sodium ethoxide. This mechanism is in accordance with experimental results. Glycerol with 5% sodium hydroxide exhibited a relevant change on its DSC curve (Fig. 2c), whereas up to 5% sodium methoxide or sodium ethoxide the sample maintained stable. In the case of sodium methoxide (Fig. 2e), it was observed a small endothermic peak

Scheme 3: Hydrodeoxygenation of glycerol by sulfuric acid

at about 135 °C (peak temperature) for mixtures with 1 and 5% sodium methoxide, which was more prominent for the glycerol with 10% sodium methoxide. For sodium ethoxide, an expressive change on the DSC curve was only observed for glycerol + 10% sodium methoxide (Fig. 2f). Therefore, the effect of sodium methoxide over glycerol was higher than sodium ethoxide.

Although the contact of glycerol with sodium hydroxide, sodium methoxide, or sodium ethoxide is inevitable, since such compounds are mixed with vegetable oil and alcohol for transesterification catalysis, their presence in glycerol-rich stream must be avoided, mainly before processes with heating employment, as distillation.

Sulfuric acid

DSC curves for glycerol + sulfuric acid (H_2SO_4) are shown in Fig. 2d, where relevant changes were also observed. During heating, pure sulfuric acid partially decomposes into its precursors, as water and sulfur trioxide (SO_3). In solutions, sulfuric acid ionizes completely to generate hydronium ions (H_3O^+), hydrogen sulfate ions (HSO_4^-), and may also dissociate into sulfate ions (SO_4^{2-}). It is also an extremely oxidizing agent, reacting quickly with several substances at high temperatures [15].

Glycerol can undergo esterification reaction while contacted with organic acids, as acetic acid, forming acyl esters as mono-, di-, and triacylglycerols [44]. The acid reacts with a hydroxyl group of glycerol forming water and monoacylglycerol. A second reaction with another hydroxyl group, of the monoacylglycerol, results in water and diacylglycerol. Finally, a third reaction with the last hydroxyl group, of the diacylglycerol, results in water and triacylglycerol [44].

In the case of sulfuric acid, it has a strong dissociation force with high dissociation constants ($pK_{a1} = -6.62$ and $pK_{a2} = 1.99$), besides being extremely hygroscopic and

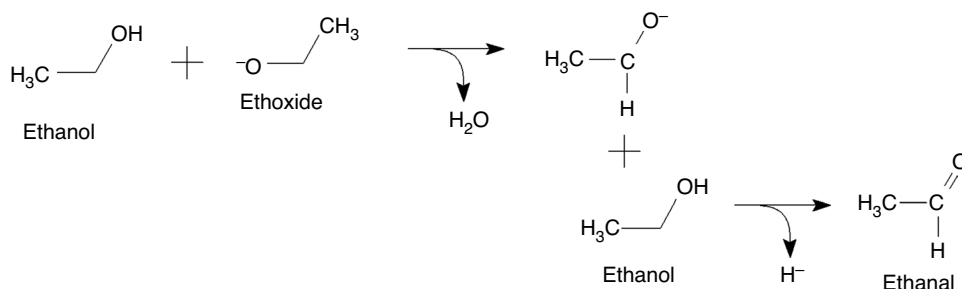
oxidative. Sulfuric acid can remove water either from the air or from many organic substances [45], as glycerol.

The presence of a strong acid as sulfuric acid may catalyze the glycerol dehydration, forming acrolein. Cheng et al. [46] obtained acrolein ($\text{C}_3\text{H}_4\text{O}$) from glycerol dehydration with 45–50 mM sulfuric acid within 335 to 380 °C. Therefore, glycerol may have been converted into acrolein during heating. Zhao et al. [47] also reported the conversion of glycerol into acrolein under acid catalyst with sulfuric acid. The dehydration of glycerol in a glycerol + water mixture (10/90 w/w) was catalyzed by 0.5 g of clay-kind powder activated by concentrated sulfuric acid. The reaction was carried out under 240 to 380 °C.

Besides acrolein, glycerol was also converted into other compounds, as hydroxyacetone ($\text{C}_3\text{H}_6\text{O}_2$), ethanal ($\text{C}_2\text{H}_4\text{O}$), and propanal ($\text{C}_3\text{H}_6\text{O}$). An increased amount of sulfuric acid in the catalyst activation led to higher acrolein yields. On the other hand, increased reaction temperature caused the generation of other compounds, mainly hydroxyacetone. However, such reactions were carried out under controlled conditions [46, 47].

Glycerol may also undergo esterification reaction, which occurs spontaneously when contacted with a strong acid. Therefore, it may have begun during sample preparation. Besides that, the reaction may have been accelerated during heating. Esterification reaction may also occur if the glycerol-rich stream contains free fatty acids carried from the transesterification or esterification reactors. In this condition, a strong acid may convert glycerol into mono-, di-, or triacylglycerols, releasing water via acid catalysis [48].

Besides those reactions, the main hypothesis for glycerol + sulfuric acid mixtures, free of water and metallic catalysts, is that the acid caused a hydrodeoxygenation of glycerol, removing a hydroxyl group from glycerol and resulting in water and different glyceryl sulfates (Scheme 3). Considering the glyceryl monosulfate, in a next step, it is also possible to generate a cyclic glyceryl sulfate (Scheme 3).

Scheme 4: Oxidation of ethanol by sodium ethoxide

Eventually, other compounds may also be generated from successive oxidation reactions, as glyceryl disulfates or trisulfate, or also a cyclic glyceryl disulfate.

Regardless of the reaction route glycerol may have undergone when contacted with sulfuric acid, its degradation was evidenced due to several changes on DSC curves. Therefore, it is crucial to avoid that the glycerol stream has any contact with such strong acid throughout the entire biodiesel production process.

Salts

DSC curves for glycerol + sodium chloride (NaCl) and + sodium sulfate (Na_2SO_4) are illustrated in Fig. 2g and h, respectively, where is notable no relevant changes on the sample's thermal behavior. Demaman et al. [49] quantified 4.38% (m/v) of sodium chloride in a crude glycerol originated from the biodiesel production. Higher salt amount can be found solubilized in glycerol depending on its water content, although sodium chloride is more soluble in glycerol than in water [50].

Glycerol with 5% sodium chloride exhibited a slight BP increasing. Faggion et al. [51] also observed an increased boiling point for glycerol + water solution with increased sodium chloride content in the mixture. Chen et al. [50] observed lower vapor pressures for glycerol, water, or glycerol + water solutions for higher salts compositions, marked by lower activity coefficients. Although water led to a higher partial pressure of glycerol, the presence of sodium chloride was associated with an increased glycerol boiling point value. Nonetheless, glycerol maintained thermally stable when contaminated with sodium chloride. The pure salt also maintained stable during the entire heating test (Fig. 2g), without melting, dissociation, or reactions noted.

For pure sodium sulfate, two endothermic peaks were formed within 220 and 260 °C (Fig. 2h). Such salt may dissociate and generate sulfur oxides (SO , SO_2 , and/or SO_3) or sodium oxide (Na_2O) [45]. However, the salt dissociation was observed by Halle and Stern [52] only at temperatures higher than 1000 °C, which may be related to the salt high purity or its drying before analysis. Despite what was observed for the pure salt, glycerol also maintained

thermally stable when contaminated with sodium sulfate. As observed for sodium chloride, higher sodium sulfate content in glycerol caused a lower change on the mixture (glycerol + salt) boiling point (Table 2).

Although there was not observed any anomaly on glycerol thermal behavior when contaminated with salts, their removal is still crucial, since salts may deposit on the bottom of decanters and columns, and cause obstruction of pipes and accessories by incrustation. Solubilized salts (ions) may be removed by ion exchanges, whereas dispersed (insoluble) salts may be removed by filtering, settling [23], or other alternative process as solid–liquid extraction [49].

Solution ethanol and sodium methoxide

Glycerol was mixed with a commercial mixture of ethanol + 21%w sodium ethoxide, and the DSC curves are shown in Fig. 2i. Such mixture is the only ternary system here evaluated. For an industrial biodiesel production, ethanol is contacted with the vegetable oil containing about 21% of catalyst mass. Therefore, the effect of such mixture over the thermal stability of glycerol was here assessed.

It was already proved that glycerol is thermally stable even at high ethanol levels (Fig. 2b). However, glycerol degradation was observed when composed of 10% sodium ethoxide in mass (Fig. 2f), as results summarized in Table 2. According to the DSC curve of sodium ethoxide solution (Fig. 2i), it is evidenced changes on the mixture composition during heating, since several peaks were formed. Expressive exothermic peaks were formed after the endothermic ones at temperature higher than 150 °C. The main hypothesis is that exothermic peaks are related to the oxidation of ethanol by sodium ethoxide (Scheme 4), resulting in acetaldehyde (ethanal) and ethanol. Secondary compounds from oxidation reactions as carboxylic acids may also be generated and affected the DSC curve. Endothermic peaks at the beginning of the DSC curve may be associated with both acetaldehyde (BP = 20.2 °C [15]) and ethanol (BP = 78.2 °C [15]) evaporation (peak temperatures under $p = 760$ mmHg).

The effects of sodium ethoxide solution over glycerol is probably the same as the ones described for glycerol + sodium ethoxide mixtures. Similar results were indeed

observed for glycerol + sodium ethoxide solution systems (Fig. 2i). Changes on sample DSC curve was observed for glycerol + 10% sodium ethoxide solution. However, such changes were less expressive than the ones observed for glycerol + 10% sodium ethoxide. Moreover, in glycerol + 10% sodium ethoxide solution there is a lower amount of the contaminant than in glycerol + 10% pure sodium ethoxide. Therefore, the oxidative effect of sodium ethoxide was less prominent. In this case, glycerol boiling peak is still observable, whereas for glycerol + 10% sodium ethoxide, it is not. In addition, the generation of other compounds as proposed in Scheme 5 may also have affected the evaporation peaks and the DSC curves.

Test 2: cycle runs

DSC curves from Test 2 are illustrated in Fig. 3 for the mixtures here evaluated. Not all mixtures evaluated in Test 1 were subjected to Test 2. Mixtures of glycerol with water or ethanol were discarded since the evaporation of such compounds caused the lid rupture, leading thus to mass losses.

Slight changes among the first cycle and the next ones are already expected in such analysis. The DSC curve generated during the first heating run is related to the properties of the material as it is at the initial conditions. From the second cycle onward, it is possible to evaluate the impact of the heating over the material properties if it is submitted again to another batch or reprocessing. If no changes were observed, the material is maintained thermally stable throughout the heating cycles.

Anomalies on DSC curves of glycerol + 10% sodium hydroxide (Fig. 3a), + 0.5% sulfuric acid (Fig. 3b), + 10% sodium methoxide (Fig. 3c), or + 10% sodium ethoxide (Fig. 3d) were observed, which were marked by the presence of exothermic or endothermic peaks. Such peaks were observed during the first heating run and are quite discrepant in relation to those slight changes expected between the first and second heating run. Therefore, they may be associated with the sample's degradation, which is consistent with the outcomes from Test 1. Finally, as observed in Test 1, glycerol + salts (Figs. 3e, f) revealed to be stable throughout Test 2.

Pure glycerol

Pure glycerol was subjected either to Test 2 or to a different cycle test. The conditions of this last test were the same as the ones described for Test 2, however the sample pan was maintained opened (without lid) during ten heating-cooling cycles within 70 and 200 °C (Fig. 1c). In this condition, glycerol was kept in contact with the atmospheric air during the entire test. After the end of each heating run, the system was cooled and the sample integrity inside the pan was thus

verified. For that, it was simply observed any change on the sample's color.

The results from DSC curves of Fig. 1b (Test 2) and Fig. 1c (Test 2 with an opened pan) proved that pure glycerol is thermally stable even when exposed to an oxidant atmosphere (air) and under local pressure (945 ± 10 hPa). Therefore, high-purity glycerol can be exposed to consecutive heating and cooling processes without resulting in its degradation. Again, slight differences among the DSC curve of the first heating run and the others are already expected, and are not associated with the compound decomposition.

Thermogravimetry analysis

Some mixtures were selected to be also subjected to the thermogravimetry (TG) to confirm the sample's degradation. The results from TG are shown in Fig. 4, where it is notable the mass declining from about 170 °C for all samples. Such mass decreasing is indeed related to the sample (glycerol) volatilization, as was observed in Test 1.

For glycerol + 10% sodium hydroxide mixture (Fig. 4a), the thermal event marked by the first tall blue peak represented 81.68% of mass loss. The remaining mass maintained inside the pan until the second thermal event at about 440 °C, where 5.36% of mass was lost. At the end of the heating run ($T=500$ °C), about 13% of the initial sample mass still remain without evaporation. Since the mixture was composed of 90% glycerol (in mass), it was expected that during the first thermal event, the mass loss was close to 90%. This should occur in a condition in which the initial glycerol mass was preserved, but not all glycerol mass was lost during its evaporation. Such observation revealed that a fraction of glycerol was consumed, resulting in other compounds of different volatility.

Nevertheless, the tall blue peak is not well formed, indicating that other thermal events are also occurring along with the glycerol evaporation. Therefore, the mass loss percentage related to this event may not be associated with only glycerol evaporation.

The same discussion can be applied to glycerol + 10% sodium methoxide mixture (Fig. 4b). Although, in this case, the thermal event was responsible for 89.5% mass loss (what was expected), the blue peak was also bad formed, indicating other events during the glycerol evaporation.

Blue peaks for glycerol + 5% sodium ethoxide (Fig. 4c) and + 10% sodium ethoxide (Fig. 4d) mixtures were better formed when compared to the ones from Fig. 4a, b. As was already discussed for oxides, the sodium ethoxide effect over glycerol is less damaging than sodium hydroxide and sodium methoxide. For glycerol + 5% sodium ethoxide mixture (Fig. 4c), the thermal event represented 94.94% of mass loss. However, for glycerol + 10% sodium ethoxide mixture (Fig. 4d), 94.53% of mass was lost during the thermal event,

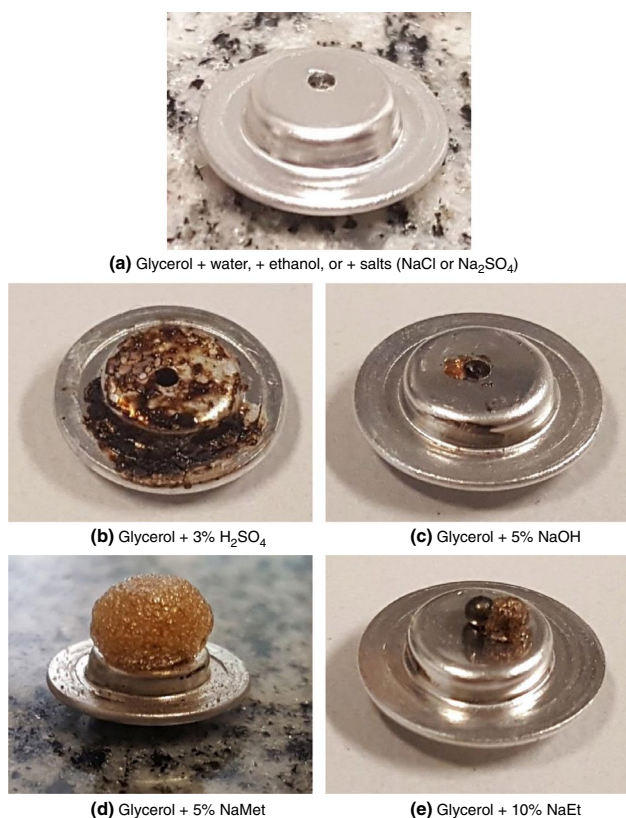


Fig. 5 Photographs of sample pans after Test 1

being that up to 90% were expected. This indicates the other thermal events were simultaneously occurring.

Finally, all of these observations revealed that glycerol undergone reactions when contacted with sodium hydroxide, sodium methoxide, or sodium ethoxide during heating and reinforce thus the outcomes from Tests 1 and 2.

Visual sample degradation

The most drastic glycerol decompositions were also visually observed (Fig. 5), from which the sample degradation was indeed confirmed. From the photographs of Fig. 5, it was confirmed that the sample pan was maintained clean after Test 1 with water or ethanol (Fig. 5a). On the other hand, sulfuric acid (Fig. 5b) and sodium hydroxide (Fig. 5c) caused a kind of corrosion, whereas a foam was formed in samples with sodium methoxide (Fig. 5d) or sodium ethoxide (Fig. 5e). The liberation of volatile compounds as previously discussed for alkoxides (sodium methoxide and sodium ethoxide) may have contributed for the foam formation. With exception of adding water, ethanol, and salts into glycerol (Fig. 5a), a combustion was observed for the other mixtures after Test 1, marked by the brown/hazel colors in Fig. 5b–e.

Conclusions

DSC and TG analyses proved to be fast and efficient tools to assess qualitative results of thermal stability of both pure and contaminated glycerol. Evaluated mixtures of glycerol with water, ethanol, and salts (sodium chloride or sodium sulfate), maintained thermally stable until the total evaporation of volatile compounds. In relation to the boiling point of pure glycerol, water caused a decreased boiling point of the mixture, which was not expressively noted for ethanol. A small increasing on the mixture boiling point was observed for increased salts composition. Glycerol containing ethanol and water is secure to be subjected to heating processes, as distillation. Consequently, purified glycerol can be employed as solvent in the extractive distillation for ethanol dehydration. The reboiler temperature can reach more than 250 °C without causing its degradation. Moreover, pure glycerol (99.5%) revealed to be thermally stable even after 10 cycles of heating and cooling.

Pure sulfuric acid, sodium hydroxide, sodium methoxide, and sodium ethoxide revealed to be thermally instable, and several compounds can be generated during heating. When present in glycerol, such compounds can compromise its quality and difficult its purification. Therefore, it is suggested to neutralize them with the proper acid or base and to remove the salts. Salts can be easily removed by settling, centrifugation, or mechanical filtering, if insoluble, or by ion exchange resins (cationic and anionic), in the case of dissociated ions.

The presence of 5% sodium hydroxide in glycerol caused the sample degradation. Although no expressive changes were observed in the mixture of glycerol with 1 or 2% sodium hydroxide, the presence of such strong alkaline compound in glycerol should be avoided. Sulfuric acid at any concentration caused an evident decomposition of glycerol. Catalysts commonly adopted in homogenous transesterification process for biodiesel production, as sodium methoxide and sodium ethoxide, also caused glycerol degradation. The effect of sodium methoxide was stronger than the one observed for sodium ethoxide. Therefore, catalysts should be also removed from glycerol before any heating process. The effect of each contaminant over glycerol was separately evaluated. Several combinations can be also evaluated. However, outcomes from pure compounds and binary mixtures provided preliminary information that can be used in further experimental assays or as control parameters in computational simulations, for instance.

Supplementary Information The online version contains supplementary material available at <https://doi.org/10.1007/s10973-022-11395-4>.

Acknowledgements The authors kindly appreciate *Conselho Nacional de Desenvolvimento Científico e Tecnológico*—CNPq (Grants

307398/2019-6, 406963/2016-9, 308924/2017-7, and 426913/2018-3), *Fundação de Amparo à Pesquisa do Estado de São Paulo*—FAPESP (Grants 2014/21252-0, 2016/10636-8, and 2018/13207-6), and *Coordenação de Aperfeiçoamento de Pessoal de Nível Superior*—CAPES (Finance Code 001) for the financial support.

References

1. Navas MB, Lick ID, Bolla PA, Casella ML, Ruggera JF. Transesterification of soybean and castor oil with methanol and butanol using heterogeneous basic catalysts to obtain biodiesel. *Chem Eng Sci*. 2018;187:444–54. <https://doi.org/10.1016/j.ces.2018.04.068>.
2. Cheng JJ, Timilsina GR. Status and barriers of advanced biofuel technologies: a review. *Renew Energy*. 2011;36:3541–9. <https://doi.org/10.1016/j.renene.2011.04.031>.
3. Sajjadi B, Raman AAA, Arandiyani H. A comprehensive review on properties of edible and non-edible vegetable oil-based biodiesel: composition, specifications and prediction models. *Renew Sustain Energy Rev*. 2016;63:62–92. <https://doi.org/10.1016/j.rser.2016.05.035>.
4. Lam MK, Lee KT, Mohamed AR. Homogeneous, heterogeneous and enzymatic catalysis for transesterification of high free fatty acid oil (waste cooking oil) to biodiesel: a review. *Biotechnol Adv*. 2010;28:500–18. <https://doi.org/10.1016/j.biotechadv.2010.03.002>.
5. UNComtrade. United Nations Commodity Trade Statistics Database. 2022. <http://comtrade.un.org/db>.
6. Simoes AJG., Hidalgo CA. The economic complexity observatory: an analytical tool for understanding the dynamics of economic development. 2022. <http://oec.world/>.
7. Sangaletti-Gerhard N, Vieira TMFDS, Groppo SS, Rodrigues JR, Regitano-d'Arce MAB. Alkaline-catalyzed ethanolysis of soybean oil ethanolic miscella. *Fuel*. 2014;116:415–20. <https://doi.org/10.1016/j.fuel.2013.08.033>.
8. Narváez PC, Noriega MA, Cadavid JG. Kinetics of palm oil ethanolysis. *Energy*. 2015;83:337–42. <https://doi.org/10.1016/j.energy.2015.02.029>.
9. Ferrero GO, Sánchez-Faba EM, Eimer GA. Two products one catalyst: emulsifiers and biodiesel production combining enzymology, nanostructured materials engineering and simulation models. *Chem Eng J*. 2018;348:960–5. <https://doi.org/10.1016/j.cej.2018.05.048>.
10. Basso RC, de Almeida Meirelles AJ, Batista EAC. Densities and viscosities of fatty acid ethyl esters and biodiesels produced by ethanolysis from palm, canola, and soybean oils: experimental data and calculation methodologies. *Ind Eng Chem Res*. 2013;52:2985–94. <https://doi.org/10.1021/ie3026899>.
11. Basso RC, Miyake FH, de Almeida Meirelles AJ, Batista EAC. Liquid–liquid equilibrium data and thermodynamic modeling, at T/K=298.2, in the washing step of ethyl biodiesel production from crambe, fodder radish and macauba pulp oils. *Fuel*. 2014;117:590–7. <https://doi.org/10.1016/j.fuel.2013.09.020>.
12. Ferreira MC, Bessa LCBA, Shiozawa S, Meirelles AJA, Batista EAC. Liquid–liquid equilibrium of systems containing triacylglycerols (canola and corn oils), diacylglycerols, monoacylglycerols, fatty acids, ester and ethanol at T/K=303.15 and 318.15. *Fluid Phase Equilib*. 2015;404:32–41. <https://doi.org/10.1016/j.fluid.2015.06.027>.
13. Souza WLR, Silva CS, Meleiro LAC, Mendes MF. Vapor–liquid equilibrium of the (water+ethanol+glycerol) system: experimental and modelling data at normal pressure. *J Chem Thermodyn*. 2013;67:106–11. <https://doi.org/10.1016/j.jct.2013.07.012>.
14. Zhang L, Yang B, Zhang W. Vapor-liquid equilibrium of water + ethanol + glycerol: experimental measurement and modeling for ethanol dehydration by extractive distillation. *J Chem Eng Data*. 2015;60:1892–9. <https://doi.org/10.1021/acs.jced.5b00116>.
15. National Center for Biotechnology Information. NCBI PubChem Database. 2022. <https://pubchem.ncbi.nlm.nih.gov>.
16. ChemSpider. Royal Society of Chemistry. Chem. Database. 2021. <http://www.chemspider.com/>.
17. Meirelles AJA, Rodrigues CEC, Gonçalves CB, Batista EAC, Katekawa ME. Processo de desacidificação de óleos e gorduras por extração líquido-líquido e processo de purificação de biodiesel e de tratamento do reagente alcoólico. Brazil: PI0900869-1 2011.
18. Piękos R, Wesolowski M, Teodorczyk J. Thermal analysis of some pharmaceutically relevant systems obtained by sol–gel technique. *J Therm Anal Calorim*. 2002;70:447–54. <https://doi.org/10.1023/A:1021672423400>.
19. Castelló ML, Dweck J, Aranda DAG. Thermal stability and water content determination of glycerol by thermogravimetry. *J Therm Anal Calorim*. 2009;97:627–30. <https://doi.org/10.1007/s10973-009-0070-z>.
20. Gomes R, Meek ME. Concise international chemical assessment document 43—ACROLEIN. Geneva: United Nations Environment Programme; International Labour Organization; World Health Organization; 2002.
21. Ji Y. Recent development of heterogeneous catalysis in the transesterification of glycerol to glycerol carbonate. *Catalysts*. 2019;9:581. <https://doi.org/10.3390/catal9070581>.
22. Kaur J, Sarma AK, Jha MK, Gera P. Valorisation of crude glycerol to value-added products: perspectives of process technology, economics and environmental issues. *Biotechnol Rep*. 2020;27:e00487. <https://doi.org/10.1016/j.btre.2020.e00487>.
23. Hájek M, Skopal F. Treatment of glycerol phase formed by biodiesel production. *Bioresour Technol*. 2010;101:3242–5. <https://doi.org/10.1016/j.biortech.2009.12.094>.
24. More GV, Rao YVH. Thermogravimetric study and combustion characteristics of biodiesel blends produced from repurpose used cooking oil. *Int J Environ Sci Technol*. 2021. <https://doi.org/10.1007/s13762-021-03474-0>.
25. More GV, Hanumantha Rao YV, Kedar SA, Gawande SH. Biodiesel production from DK oils using Taguchi L9 techniques: characterization and thermogravimetric study of combustion characteristics. *J Therm Anal Calorim*. 2021. <https://doi.org/10.1007/s10973-021-11020-w>.
26. Barbeiro LB, Matricarde Falleiro RM, Meirelles AJA. Vapor pressure and VLE data of fatty compounds. *J Chem Thermodyn*. 2021;159:106469. <https://doi.org/10.1016/j.jct.2021.106469>.
27. ASTM. E967-08: standard test method for temperature calibration of differential scanning calorimeters and differential thermal analyzers. New York: American Society for Testing and Materials; 2010. <https://doi.org/10.1520/E0967-08R14.2>.
28. ASTM. E968-02: standard practice for calibration of fixed-cell differential scanning calorimeters. New York: American Society for Testing and Materials; 2010. <https://doi.org/10.1520/E0968-02R14.2>.
29. Silva LYA, Falleiro RMM, Meirelles AJA, Krähenbühl MA. Determination of the vapor pressure of ethyl esters by differential scanning calorimetry. *J Chem Thermodyn*. 2011;43:943–7. <https://doi.org/10.1016/j.jct.2011.01.017>.
30. Falleiro RMM, Silva LYA, Meirelles AJA, Krähenbühl MA. Vapor pressure data for fatty acids obtained using an adaptation of the DSC technique. *Thermochim Acta*. 2012;547:6–12. <https://doi.org/10.1016/j.tca.2012.07.034>.
31. Taylor BN, Kuyatt CE. Guidelines for evaluating and expressing the uncertainty of NIST measurement results. NIST Tech Note 1297. United States Department of Commerce Technology Administration; 1994. p. 1–20.

32. Silva LYA, Falleiro RMM, Meirelles AJA, Krähenbühl MA. Vapor–liquid equilibrium of fatty acid ethyl esters determined using DSC. *Thermochim Acta*. 2011;512:178–82. <https://doi.org/10.1016/j.tca.2010.10.002>.
33. Falleiro RMM, Meirelles AJA, Krähenbühl MA. Experimental determination of the (vapor+liquid) equilibrium data of binary mixtures of fatty acids by differential scanning calorimetry. *J Chem Thermodyn*. 2010;42:70–7. <https://doi.org/10.1016/j.jct.2009.07.008>.
34. National Oceanic and Atmospheric Administration (NOAA). CAMEO Chemicals. Database of Hazardous Materials. 2022. <http://cameochemicals.noaa.gov>.
35. Nakagawa H, Oyama T. Molecular basis of water activity in glycerol-water mixtures. *Front Chem*. 2019;7:1–9. <https://doi.org/10.3389/fchem.2019.00731>.
36. Jahn DA, Akinkunmi FO, Giovambattista N. Effects of temperature on the properties of glycerol: a computer simulation study of five different force fields. *J Phys Chem B*. 2014;118:11284–94. <https://doi.org/10.1021/jp5059098>.
37. SDA - The Soap and Detergent Association. Glycerine: an overview. New York: Glycerine & Oleochemical Division; 1990.
38. Li K-T, Li H-H. Glycerol conversion to lactic acid with unsupported copper salts and bulk cupric oxide in aqueous alkali media. *Appl Biochem Biotechnol*. 2020;191:125–34. <https://doi.org/10.1007/s12010-020-03237-6>.
39. Torres A, Shi H, Subramaniam B, Chaudhari RV. Aqueous-phase glycerol catalysis and kinetics with in situ hydrogen formation. *ACS Sustain Chem Eng*. 2019;7:11323–33. <https://doi.org/10.1021/acssuschemeng.9b00807>.
40. Song D, Rochelle GT. Reaction kinetics of carbon dioxide and hydroxide in aqueous glycerol. *Chem Eng Sci*. 2017;161:151–8. <https://doi.org/10.1016/j.ces.2016.11.048>.
41. Yurkinskii VP, Firsova EG, Proskura SA. Thermal dissociation of sodium hydroxide upon evacuation. *Inorg Synth Ind Inorg Chem*. 2005;78:360–2. <https://doi.org/10.1007/s11167-005-0296-x>.
42. International Chemical Safety Cards. ICSC 0771—sodium meth-ylate. Geneva: International Labour Organization; World Health Organization; 2009.
43. Chandran K, Kamruddin M, Ajikumar PK, Gopalan A, Ganesan V. Kinetics of thermal decomposition of sodium methoxide and ethoxide. *J Nucl Mater*. 2006;358:111–28. <https://doi.org/10.1016/j.jnucmat.2006.07.003>.
44. Okoye PU, Hameed BH. Review on recent progress in catalytic carboxylation and acetylation of glycerol as a byproduct of bio-diesel production. *Renew Sustain Energy Rev*. 2016;53:558–74. <https://doi.org/10.1016/j.rser.2015.08.064>.
45. PubChem. Hazardous Substances Data Bank (HSDB). National Center for Biotechnology Information. 2022. <https://www.nlm.nih.gov/toxnet/index.html>.
46. Cheng L, Liu L, Ye XP. Acrolein production from crude glycerol in sub- and super-critical water. *J Am Oil Chem Soc*. 2013;90:601–10. <https://doi.org/10.1007/s11746-012-2189-5>.
47. Zhao H, Zhou CH, Wu LM, Lou JY, Li N, Yang HM, et al. Catalytic dehydration of glycerol to acrolein over sulfuric acid-activated montmorillonite catalysts. *Appl Clay Sci*. 2013;74:154–62. <https://doi.org/10.1016/j.clay.2012.09.011>.
48. Savaliya ML, Dholakiya BZ. Cellulose sulfuric acid catalyzed esterification of biodiesel derived raw glycerol to medium chain triglyceride: the dual advantage. *Catal Lett*. 2014;144:1399–406. <https://doi.org/10.1007/s10562-014-1275-8>.
49. Demaman Oro CE, Bonato M, Oliveira JV, Tres MV, Mignoni ML, Dallago RM. A new approach for salts removal from crude glycerin coming from industrial biodiesel production unit. *J Environ Chem Eng*. 2019;7: 102883. <https://doi.org/10.1016/j.jece.2019.102883>.
50. Chen DHT, Thompson AR, Chen DHT. Isobaric vapor–liquid equilibria for the systems glycerol–water and glycerol–water saturated with sodium chloride. *J Chem Eng Data*. 1970;15:471–4. <https://doi.org/10.1021/je60047a019>.
51. Faggion H, Gaschi PS, Corazza ML, Cardozo-Filho L, Igarashi-Mafra L, Mafra MR. NaCl and KCl effect on (vapour+liquid) equilibrium of binary, ternary and quaternary systems involving water, ethanol and glycerol at low pressures. *J Chem Thermodyn*. 2016;98:95–101. <https://doi.org/10.1016/j.jct.2016.02.026>.
52. Halle JC, Stern KH. Vaporization and decomposition of sodium sulfate. *Thermodynamics and kinetics*. *J Phys Chem*. 1980;84:1699–704. <https://doi.org/10.1021/j100450a007>.

Publisher's Note Springer Nature remains neutral with regard to jurisdictional claims in published maps and institutional affiliations.

Authors and Affiliations

Daniel Gonçalves^{1,2}  · Lilian Bozzi Barbeiro² · Patrícia Tonon de Souza² · Eduardo Augusto Caldas Batista² · Antonio José de Almeida Meirelles² 

✉ Daniel Gonçalves
danielg@uenf.br

✉ Antonio José de Almeida Meirelles
tomze@unicamp.br

¹ Present Address: Laboratory of Food Technology (LTA), Universidade Estadual do Norte Fluminense Darcy Ribeiro (UENF), 2000 Alberto Lamego Ave., Campos dos Goytacazes, RJ 28013-602, Brazil

² Laboratory of Extraction, Applied Thermodynamics, and Equilibrium (ExTrAE), Department of Food Engineering and Technology (DETA), School of Food Engineering (FEA), University of Campinas (UNICAMP), 80 Monteiro Lobato St., Campinas, SP 13083-862, Brazil